UDC 620.181 : 669
https://doi.org/10.17073/0021-3438-2024-1-42-54

Research article
Научная статья

Effects of quenching temperature on the structure, segregation, and properties of the AM4.5Kd + 0.2 wt.% La alloy after artificial aging

N.A. Slavinskaya, H. Ri, E.H. Ri, A.S. Zhivetev

Pacific National University
136 Tikhookeanskaya Str., Khabarovsk 680035, Russia

✉ Andrei S. Zhivetev (007881@pnu.edu.ru)

Abstract: The identification of structural components in the AM4.5Kd + 0.2 wt.% La alloy, subjected to quenching at different temperatures (535–605 °C) and artificial aging at 155 °C for 4 h, was conducted through electron microscopy and XRD. An increase in the quenching temperature (t_q) from 535 to 605 °C promotes the enlargement of structural components, including the α-solid solution, various aluminides, and eutectics. We observed that the base metal is not homogeneous in its chemical composition, consisting of two types of solid solutions: α_1 and α_2. The Cu and Mn solubility in the α_2-solid solution is higher than in the α_1-solid solution. As the quenching temperature increases to t_q = 605 °C, the copper content in the α_1-solid solution decreases. In contrast, the copper content in the α_2-solid solution follows a curve with two maxima at 545 °C (4.5 at.%) and 585 °C (8.7 at.%). The Mn content in the α_1-solid solution decreases sharply to the 545 °C quenching temperature and remains relatively constant up to t_q = 605 °C (0.2 at.%). The Mn content in the α_2-solid solution follows a curve with its maximum at t_q = 545 °C (4.3 at.% Mn). Subsequent temperature rise results in a sharp drop in Mn content from 1.0 at.% at t_q = 565 °C to 0.3 at.% at 605 °C. Hence, the max solubility of Cu and Mn in the α_2-solid solution occurs at 545 °C. At 585 °C, only an elevated Cu content (~8.7 at.%) was observed. Aluminides of alloying elements with different stoichiometries crystallize at different quenching temperatures, with complex $Al_xTi_yLa_zCu_vCd_w$ and $Al_xCu_yMn_zCd_v$ alloyed aluminides being most commonly found. ncreasing the quenching temperature to 535–545 °C results in higher hardness of the AM4.5Kd + 0.2 wt.% of La alloy, reaching 98–104 HB, with subsequent decrease to 60 HB as the quenching temperature reaches 605 °C. The hardness of the unhardened alloy is 60 HB. The optimal quenching temperature for the AM4.5Kd + 0.2 wt.% of La alloy is in the range of 535–545 °C. This temperature corresponds to the highest hardness of the alloy and the microhardness of the aluminide.

Keywords: AM4.5Kd aluminum alloy, La addition, quenching, aging, phase composition, aluminides, hardness, microhardness.

For citation: Slavinskaya N.A., Ri H., Ri E.H., Zhivetev A.S. The influence of tempering temperature conditions on the formation of the structure, liquation processes and properties of the alloy AM4.5Kd + 0.2 wt.% La after artificial aging. *Izvestiya. Non-Ferrous Metallurgy.* 2024;30(1):42–54. https://doi.org/10.17073/0021-3438-2024-1-42-54

Влияние температурных режимов закалки на формирование структуры, ликвационные процессы и свойства сплава АМ4,5Кд + 0,2 мас.% La после искусственного старения

Н.А. Славинская, Х. Ри, Э.Х. Ри, А.С. Живетьев

Тихоокеанский государственный университет
Россия, 680035, г. Хабаровск, ул. Тихоокеанская, 136

✉ Андрей Сергеевич Живетьев (007881@pnu.edu.ru)

Аннотация: Методами электронно-микроскопического исследования и микрорентгеноспектрального анализа элементов идентифицированы структурные составляющие сплава АМ4,5Кд + 0,2 мас.% La после закалки с различных температур (t = 535÷605 °С) и искусственного старения при t = 155 °С в течение 4 ч. Повышение температуры закалки от 535 до 605 °С способствует укрупнению структурных составляющих – α-твердого раствора, алюминидов различного состава, эвтектики. Установлено, что металлическая основа неоднородна по химическому составу и состоит из двух видов твердого раствора – α_1 и α_2. В α_2-твердом растворе растворяются в большей степени Cu и Mn, по сравнению с α_1-твердым раствором. С увеличением температуры закалки до 605 °С содержание меди в α_1-твердом растворе уменьшается, в то же время в α_2-твердом растворе концентрация меди изменяется по экстремальной зависимости с двумя ее максимумами при температурах 545 °С (4,5 ат.%) и 585 °С (8,7 ат.%). Содержание марганца в α_1-твердом растворе резко снижается до температуры закалки 545 °С, а затем остается без изменения до t = 605 °С (0,2 ат.%). Содержание марганца в α_2-твердом растворе изменяется также по экстремальной зависимости с максимумом концентрации при t = 545 °С (4,3 ат.% Mn). Дальнейшее повышение температуры закалки способствует резкому уменьшению содержания марганца от 1,0 ат.% при t = 565 °С до 0,3 ат.% Mn при температуре закалки 605 °С. Таким образом, максимальная растворимость Cu и Mn в α_2-твердом растворе наблюдается при температуре закалки 545 °С. При температуре закалки 585 °С фиксируется только повышенное содержание меди (~8,7 ат.%). В зависимости от температуры закалки кристаллизуются алюминиды легирующих элементов с различной стехиометрией. Наиболее часто встречаются комплексно-легированные алюминиды титана $Al_xTi_yLa_zCu_vCd_w$ и меди $Al_xCu_yMn_zCd_v$. Увеличение температуры закалки до 535–545 °С способствует росту твердости сплава АМ4,5Кд + 0,2 мас.% La до 98–104 НВ с последующим ее снижением (60 НВ) до температуры закалки 605 °С. Сплав без термической обработки имел твердость 60 НВ. Оптимальный режим закалки сплава АМ4,5Кд + 0,2 мас.% La соответствует температуре 535–545 °С, при которой наблюдаются максимальные твердость сплава и микротвердость интерметаллида.

Ключевые слова: алюминиевый сплав АМ4,5Кд, модифицирование La, закалка, искусственное старение, фазовый состав, алюминиды, твердость, микротвердость.

Для цитирования: Славинская Н.А., Ри Х., Ри Э.Х., Живетьев А.С. Влияние температурных режимов закалки на формирование структуры, ликвационные процессы и свойства сплава АМ4,5Кд + 0,2 мас.% La после искусственного старения. *Известия вузов. Цветная металлургия*. 2024;30(1):42–54.
https://doi.org/10.17073/0021-3438-2024-1-42-54

Introduction

The enhancement of aluminum alloys, both at standard and elevated temperatures, is frequently employed to manufacture dependable and durable components for the aerospace and automotive industries [1]. Their strength characteristics closely resemble those of gray cast iron and carbon steel [2]. However, it is noteworthy that aluminum alloys exhibit lower wear resistance compared to the latter materials [3; 4].

It has been established that Al—Cu alloys exhibit high heat resistance, as exemplified by the AM5 casting alloy (GOST 1583—93) and the deformable alloys 1201, D16, and AK4—1 (GOST 4784—97). Nevertheless, their heat resistance is sustained only up to temperatures of 200—250 °C [2].

A comprehensive literature review indicates that heat treatment (HT) of aluminum alloys is often the sole viable method for achieving the necessary mechanical properties and creating the desired structures in the alloy [5—11]. Previous works, such as those presented in references [5; 8], propose optimal heat treatment procedures aimed at enhancing the mechanical properties [11] of Al—Cu—Mg alloys. Additionally, Korotkova N. et al. [7]

investigated the correlation between the structure of aluminum wire with a 7 % rare earth metal (REM) content and the annealing temperature within the 300—600 °C range.

The impact of heat treatment conditions on the structure and mechanical performance of Al—Mg alloys is systematically assessed in works cited in references [6; 9].

Certain researchers [12—14] employ simulation techniques to model heat treatment processes. Notably, papers [15—17] showcase a notable concordance between the simulated structure, properties, and processes in the Al—Cu—Cd alloy and the corresponding experimental data.

Alloying additives play a crucial role in modifying and controlling the structure and properties of alloys [1; 18—29]. Among the frequently utilized alloying additives, Ti and B are prominent. Research studies [18; 19; 22—24] indicate that these additives alter the morphology of the dendritic α-Al phase, promote the formation of equiaxed grains, and establish new nucleation sites for Ti and B compounds. This leads to a substantial refinement of the alloy structure, resulting in improved mechanical properties. Furthermore, the incorporation of REEs and transition group metals (up to 1 wt.%) enhances the structure of aluminum alloys post-casting and heat treatment. Sahin H. et al. [20] observed that additions of Er and Eu reduce the size of intermetallic phases, while the addition of 0.1 wt.% Sc increases the nanohardness of certain intermetallic compounds [21]. Additionally, the introduction of Ce (up to 0.5 %) diminishes the size of β-Al_5FeSi inclusions from 51 to 21 μm [29]. Andrushevich A. et al [25] remark that the addition of Sr to the AK7h alloy enhances its mechanical properties and influences casting characteristics. This alteration in the solidification pattern disperses pores, positively impacting the tightness of housing parts.

Ri E. et al. [30] conducted a study examining the impacts of metallic lanthanum and cerium additions on the alloy structure, segregation, hardness, and microhardness of the AM4.5Kd (VAL 10) cast alloy. Their findings revealed that lanthanum plays a role in refining the alloy structure, redistributing elements, and augmenting microhardness.

In contrast to aluminum—silicon alloys, the influence of REEs, particularly lanthanum, on the structure, segregation, and properties of the AM4.5Kd cast alloy has not been thoroughly investigated. The components of the AM4.5Kd alloy typically undergo heat treatment involving quenching and aging. The exploration of the synergistic effects of alloying and heat treatment is both theoretically and practically significant.

The objective of this study is to ascertain the impact of quenching temperatures (535, 545, 565, 585, 605 °C) on the structure, segregation, and properties of the AM4.5Kd alloy, which incorporates 0.2 wt.% of lanthanum, following combined heat treatment involving quenching and aging.

Materials and methods

The AM4.5Kd (VAL10) alloy, conforming to GOST 1583-93, was the subject of our investigation. The alloy, weighing 0.7 kg, was melted along with additives in a Graficarbo furnace. The initial AM4.5Kd alloy was loaded into a pre-heated graphite crucible at 450 °C, followed by heating to a temperature of 740 °C. The melting process included a 5-minute holding period to stabilize the temperature within the required range. Subsequently, metallic lanthanum (LaM-1), wrapped in aluminum foil, was introduced. The additional 5-minute holding time ensured a uniform distribution of lanthanum within the alloy. This was succeeded by reheating to 740 °C, another 5-minute holding period, and the casting process. All operations were conducted in an argon environment. Casting was performed using a metal mold with a diameter of 30 mm and a height of 50 mm.

Patel N. et al. [5] proposed the following heat treatment parameters for the AM4.5Kd (VAL 10) cast alloy: T5 heat treatment, involving a temperature range of 545^{+3}_{-5}, with a holding time of 10—14 h, followed by water cooling in the range of 20 to 100 °C. In our study, we employed the following treatment protocol: heating for quenching (to temperatures of 535, 545, 565, 585, 605 °C); holding for 2.5 h, quench hardening in water (at 20 °C), and aging at a temperature of 155 °C for 4.0 h.

The average chemical composition after melting was as following (%): Al: 94.62; Cu: 4.3; Mn: 0.55; Ti: 0.19; La: 0.17; Si: 0.1; Fe: 0.07.

For microstructural analysis, we utilized a FE-SEM Hitachi Su70 (Japan) field emission scanning electron microscope equipped with Thermo Fisher Scientific MagnaRay spectrometers for energy and wave dispersion *X*-ray analysis.

Microhardness measurements (HV) were conducted using the Vickers hardness test method (in accordance with GOST 2999-75 and 9450-76) with a Shimadzu HMV-G microhardness tester (Japan).

Results and discussion

Our investigation focused on examining the impact of quenching temperatures (535, 545, 565, 585,

and 605 °C) on the structure, segregation, microhardness of structural components, and overall hardness of the AM4.5Kd alloy with an additional 0.2 wt.% of La. The subsequent aging process at 155 °C was maintained for 4 h.

The SEM analysis of the alloy structure revealed that elevated quenching temperatures contribute to the enlargement of structural components within the α-solid solution and metal aluminides, as depicted in Fig. 1.

At a quenching temperature of t_q = 565 °C and above, interfaces of the α-solid solution become evident. Additionally, spherical intermetallic inclusions crystallize within the grains of the α-solid solution.

XRD microanalysis allowed for the identification of structural components that crystallized at different quenching temperatures and subsequent aging.

Let us examine the results for two specific quenching temperatures: 545 °C (Figs. 2, 3, and Table 1) and 605 °C (Fig. 4 and Table 2). At these temperatures, structural

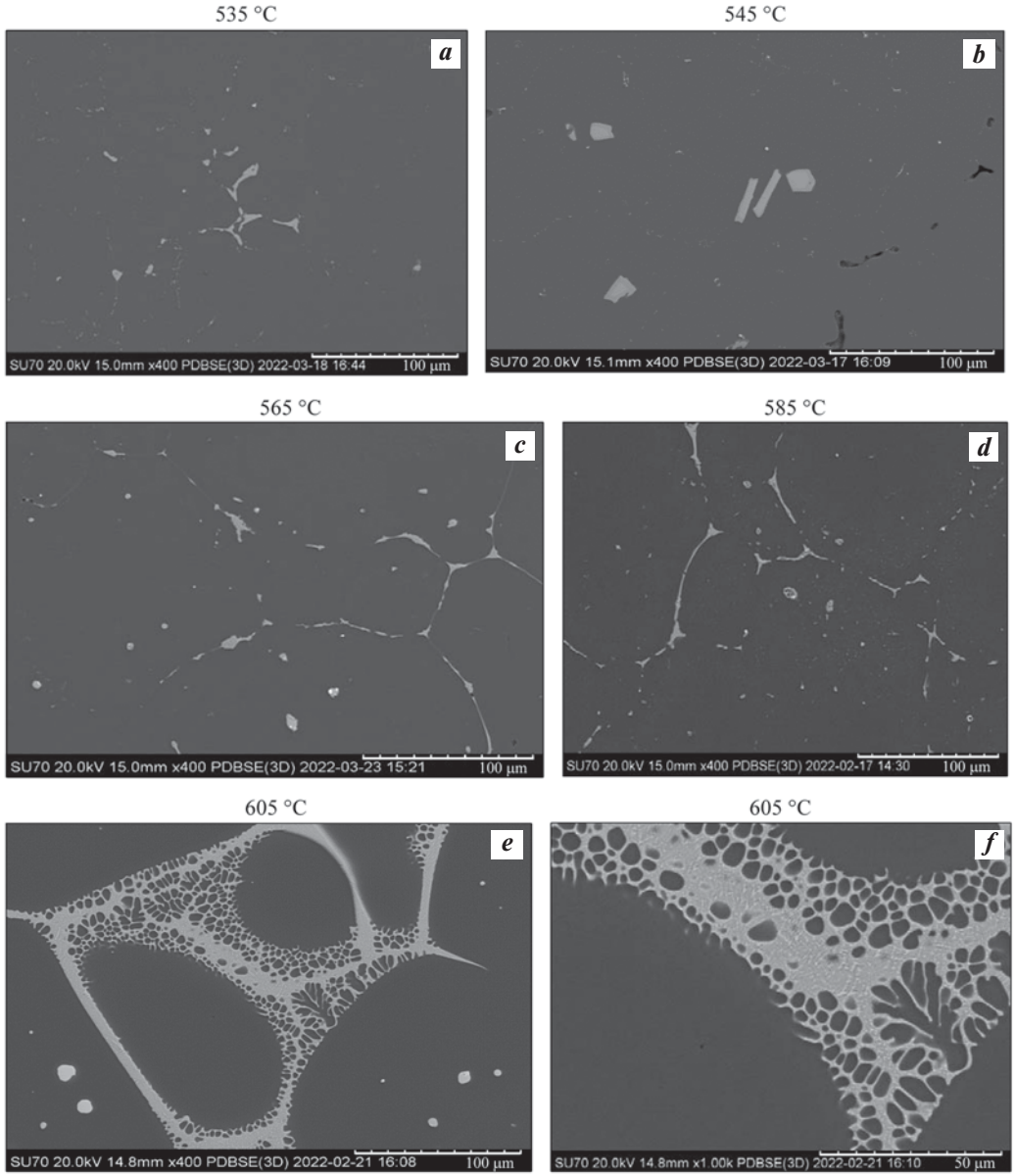

Fig. 1. Microstructure of the AM4.5Kd + 0.2 wt.% of La alloy vs. the quenching temperature (t_q) and after aging at 155 °C

t_q, °C: 535 (***a***), 545 (***b***), 565 (***c***), 585 (***d***), 605 (***e***, ***f***)

Рис. 1. Микроструктура сплава АМ4,5Кд + 0,2 мас.% La в зависимости от температуры закалки ($t_з$) и после искусственного старения при температуре 155 °C

$t_з$, °C: 535 (***a***), 545 (***b***), 565 (***c***), 585 (***d***), 605 (***e***, ***f***)

Table 1. **Composition of the structural components of AM4.5Kd alloy + 0.2 wt.% of La after quenching (545 °C) and subsequent aging (155 °C)**

Таблица 1. Состав структурных составляющих сплава АМ4,5Кд + 0,2 мас.% La после закалки (545 °C) и последующего искусственного старения (155 °C)

Structural components	Elemental analysis points (see Fig. 2)	Content, at.%						
		Al	Ti	Mn	Fe	Cu	Cd	La
α_1 solid solution of Cu, Mn, and Ti in Al	*11–17*	97.45	0.15	0.33	–	2.27	–	–
α_2 solid solution of Cu, Mn, and Fe in Al	*8–10*	89.8	–	4.25	1.22	4.7	0.08	0.46
$Al_{5.45}$(Ti, La, Cd, Cu) alloyed aluminide	*2–6*	84.5	8.52	–	–	0.95	1.63	3.41
		$Al_{84.5}(Ti, La, Cd, Cu)_{15.5} = Al_{5.45}(Ti, La, Cd, Cu)$						
$Al_{5.5}$(Cu, La, Mn, Fe) alloyed aluminide	*1*	84.6	–	1.56	0.33	9.82	–	3.68
		$Al_{84.6}(Cu, La, Mn, Fe)_{15.4} = Al_{5.5}(Cu, La, Mn, Fe)$						

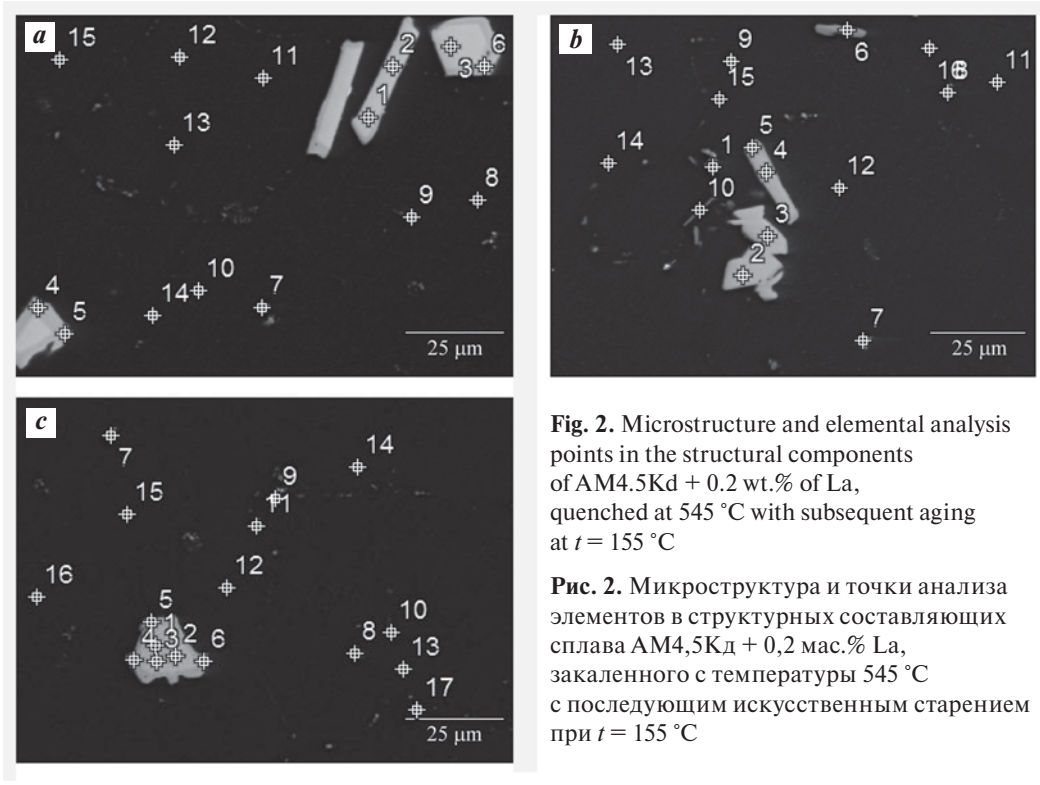

Fig. 2. Microstructure and elemental analysis points in the structural components of AM4.5Kd + 0.2 wt.% of La, quenched at 545 °C with subsequent aging at t = 155 °C

Рис. 2. Микроструктура и точки анализа элементов в структурных составляющих сплава АМ4,5Кд + 0,2 мас.% La, закаленного с температуры 545 °C с последующим искусственным старением при t = 155 °C

changes occur, leading to the formation of various metal aluminides

In Figs. 2, 3, and Table 1, the results reveal that at t_q = 545 °C, the following structures are formed: α_1 and α_2 solid solutions, as well as $Al_{5.45}$(Ti, La, Cd, Cu) and $Al_{5.5}$(Cu, La, Mn, Fe) aluminides. The crystals of the alloyed aluminide $Al_{5.45}$(Ti, La, Cd, Cu) exhibit a compact morphology resembling either polyhedra or plates, with a width in the range of several microns and a length approximately measuring 25—30 μm.

The presence of these structures is affirmed by the element distribution curves within the structural components of the AM4.5Kd + 0.2 wt.% of La alloy, quenched at 545 °C with subsequent aging. The curves follow the *A—A* line, as illustrated in Fig. 3.

In the structure of the AM4.5Kd + 0.2 wt.% of La alloy, quenched at 605 °C with subsequent aging (Fig. 4 and Table 2), similar crystallized aluminides are observed, differing in their stoichiometry: $Al_{6.0}$(Ti, La, Cu, Cd) and $Al_{3.83}$(Cu, La, Ti, Cd, Mn). Additionally, the $Al_{3.63}$(Cu, La, Mn, Fe) aluminide

is crystallized, with its crystals either forming part of the eutectics (Fig. 4, points *5—7*, (*a*), *1—3* (*b*), *9—11* (*c*)) or appearing as light, spherical inclusions (points *1—2* (*c*)).

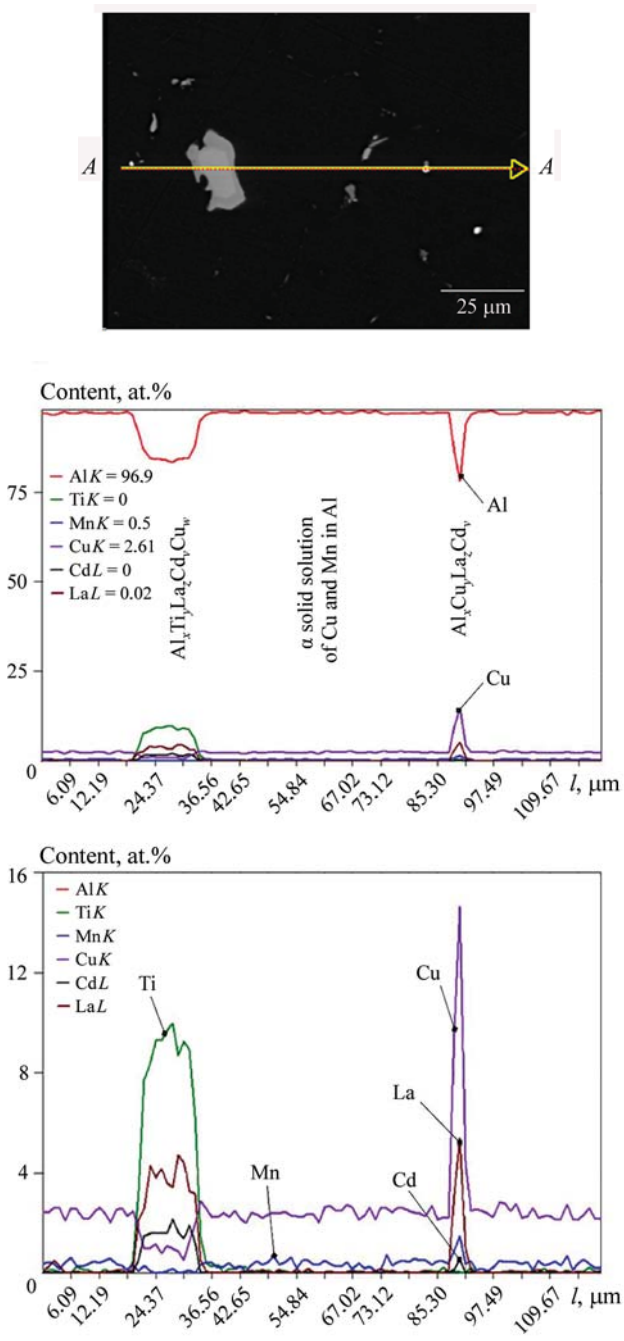

Fig. 3. Element distribution curves in the structural components of the AM4.5Kd + 0.2 wt.% of La alloy quenched at 545 °C with subsequent aging, along the *A–A* line

Рис. 3. Кривые распределения элементов в структурных составляющих сплава АМ4,5Кд + 0,2 мас.% La, закаленного с температуры 545 °С с последующим искусственным старением, по направлению профиля *А–А*

Table 3 and Fig. 5 reveal that the base metal (α-solid solution) exhibits not-homogeneity in its chemical composition, comprising two types of solid solutions: α_1 and α_2.

As the quenching temperature increases to 605 °C, the copper content in the α_1-solid solution decreases, while the copper content in the α_2-solid solution follows a curve with two maxima at t_q = 545 and 585 °C.

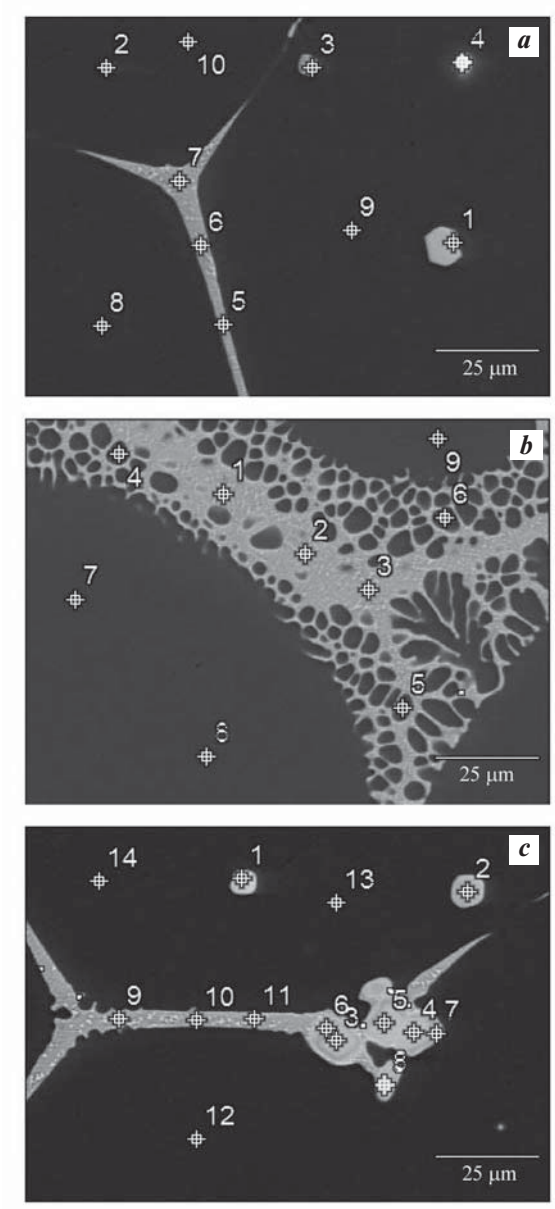

Fig. 4. Microstructure and elemental analysis points in the structural constituents of the AM4.5Kd + 0.2 wt.% of La alloy, quenched at 605 °C with subsequent aging at t = 155 °C

Рис. 4. Микроструктура и точки анализа элементов в структурных составляющих сплава АМ4,5Кд + 0,2 мас.% La, закаленного с температуры 605 °С с последующим искусственным старением при t = 155 °С

The total copper content in the solid solutions varies similarly. The aluminum content is inversely related to the solubility of copper in the α-solid solution. The content of Al in the α_1-solid solution increases monotonically to t_q = 605 °C (Fig. 5, *a*).

The content of Mn in the α_1-solid solution experiences a rapid decrease until t_q = 545 °C and remains relatively constant up to t_q = 605 °C (Fig. 5, *b*). In contrast, the content of Mn in the α_2-solid solution follows a curve with a maximum at t_q = 545 °C, decreasing thereafter

Table 2. **Composition of the structural components of AM4.5Kd alloy + 0.2 wt.% of La after quenching (605 °C) and subsequent aging (155 °C)**

Таблица 2. Состав структурных составляющих сплава АМ4,5Кд + 0,2 мас.% La после закалки (605 °C) и последующего искусственного старения (155 °C)

Structural components	Elemental analysis points (see Fig. 4)	Content, at.%						
		Al	Ti	Mn	Fe	Cu	Cd	La
α_1 solid solution of Cu, Mn, and Ti in Al	*8–10* (***a***) *7–9* (***b***) *12–14* (***c***)	98.2	0.11	0.44	–	1.27	–	–
α_2 solid solution of Cu, Mn, and Ti in Al	*4–6* (***b***)	95.7	–	0.7	–	3.94	–	–
$Al_{3.63}$(Cu, Cd, Mn, Fe) alloyed aluminide	*5–7* (***a***) *1–3* (***b***) *9–11* (***c***) *1–2* (***c***)	78.4	–	0.32	0.27	20.5	0.5	–
		$Al_{78.4}(Cu, Cd, Mn, Fe)_{21.6} = Al_{3.63}(Cu, Cd, Mn, Fe)$						
$Al_{3.83}$(Cu, La, Ti, Cd, Mn) alloyed aluminide	*1–2* (***a***)	79.3	1.23	0.48	–	13.5	0.21	5.32
		$Al_{79.3}(Cu, La, Ti, Cd, Mn)_{20.7} = Al_{3.83}(Cu, La, Ti, Cd, Mn)$						
$Al_{6.0}$(Ti, La, Cu, Cd) alloyed aluminide	*3–8* (***c***)	85.7	8.6	–	–	1.27	0.41	3.98
		$Al_{85.7}(Ti, La, Cu, Cd)_{14.3} = Al_{6.0}(Ti, La, Cu, Cd)$						

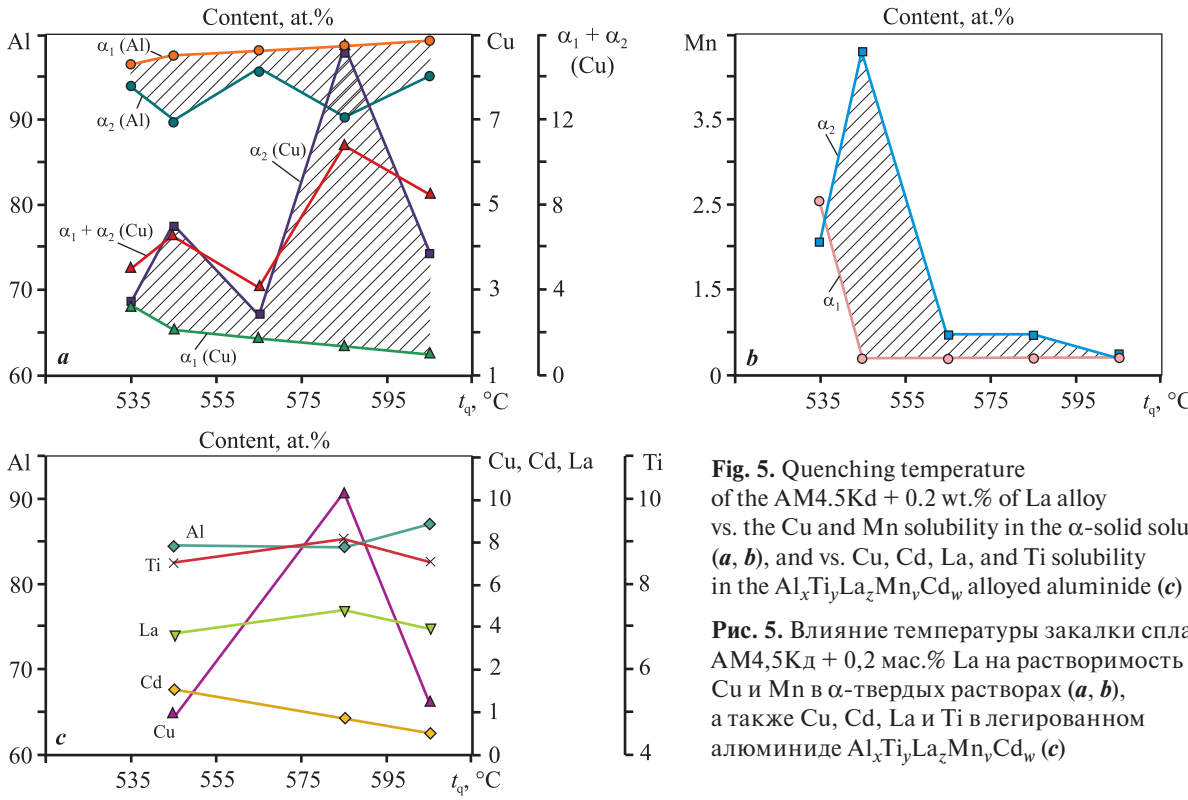

Fig. 5. Quenching temperature of the AM4.5Kd + 0.2 wt.% of La alloy vs. the Cu and Mn solubility in the α-solid solutions (***a***, ***b***), and vs. Cu, Cd, La, and Ti solubility in the $Al_xTi_yLa_zMn_vCd_w$ alloyed aluminide (***c***)

Рис. 5. Влияние температуры закалки сплава АМ4,5Кд + 0,2 мас.% La на растворимость Cu и Mn в α-твердых растворах (***a***, ***b***), а также Cu, Cd, La и Ti в легированном алюминиде $Al_xTi_yLa_zMn_vCd_w$ (***c***)

Table 3. **Elemental composition (at.%) in the structural components of the AM4.5Kd + 0.2 wt.% of La alloy vs. the quenching temperature with subsequent aging**

Таблица 3. Содержание элементов (ат.%) в структурных составляющих сплава АМ4,5Кд + 0,2 мас.% La в зависимости от температуры закалки с последующим старением

t_q, °C	α_1 solid solution	α_2 solid solution	$Al_xCu_yMn_zFe_v$	$Al_xCu_yMn_zLa_vCd_w$	$Al_xTi_yLa_zCu_vCd_w$	$Al_xCu_yLa_zMn_vFe_w$	$Al_xCu_yTi_zMn_v$	$Al_xCu_yMn_zFe_vCd_wLa$	$Al_xCu_yCd_zMn_vFe_w$
535	97.1 Al 0.31 Mn 2.55 Cu $\alpha_1 + \alpha_2 = 5.13$ Cu $\alpha_1 + \alpha_2 = 2.67$ Mn	93.3 Al 2.12 Mn 0.28 Fe 2.58 Cu	74.38 Al 0.1 Mn 24.62 Cu 0 Fe **$Al_{2.9}$(Cu, Mn)**	85.35 Al 1.2 Mn 0.16 Fe 1.54 Cu 1.75 La 0.09 Cd **$Al_{5.83}$(Cu, La, Mn, Fe)**	–	–	–	–	–
545	97.45 Al 0.15 Ti 0.33 Mn 2.07 Cu $\alpha_1 + \alpha_2 = 6.77$ Cu $\alpha_1 + \alpha_2 = 4.58$ Mn	89.4 Al 4.25 Mn 1.22 Fe 4.7 Cu 0.46 La	–	–	84.5 Al 8.52 Ti 0.95 Cu 1.63 Cd 3.41 La **$Al_{5.45}$(Ti, La, Cu, Cd)**	84.6 Al 1.56 Mn 0.33 Fe 9.82 Cu 3.68 La **$Al_{5.5}$(Cu, La, Mn, Fe)**	–	–	–
565	97.65 Al 0.12 Ti 0.25 Mn 1.98 Cu $\alpha_1 + \alpha_2 = 4.27$ Cu $\alpha_1 + \alpha_2 = 1.03$ Mn	96.96 Al 0.78 Mn 2.26 Cu	–	80.9 Al 1.55 Mn 13.44 Cu 0.32 Cd 3.5 La **$Al_{4.24}$(Cu, La, Mn)**	–	81.6 Al 7.9 Mn 1.32 Fe 9.05 Cu 0.15 La **$Al_{4.4}$(Cu, Mn, Fe, La)**	–	–	–
585	97.80 Al 0.365 Mn 1.93 Cu $\alpha_1 + \alpha_2 = 10.77$ Cu $\alpha_1 + \alpha_2 = 1.22$ Mn	90.2 Al 0.85 Mn 0.09 Fe 8.84 Cu	72.5 Al 0.11 Mn 0.22 Fe 27.2 Cu **$Al_{2.64}$(Cu, Fe, Mn)**	–	84.8 Al 9.1 Ti 10.9 Cu 0.73 Cd 4.28 La **$Al_{5.6}$(Ti, Cu, La, Cd)**	–	80.5 Al 9.09 Ti 1.18 Mn 9.22 Cu **$Al_{4.12}$(Cu, Ti, Mn)**	78.3 Al 1.84 Mn 0.26 Fe 15.18 Cu 0.37 Cd 4.03 La **$Al_{3.6}$(Cu, La, Cd, Fe, Mn)**	–
605	98.2 Al 0.11 Ti 0.44 Mn 1.27 Cu $\alpha_1 + \alpha_2 = 5.21$ Cu $\alpha_1 + \alpha_2 = 0.44$ Mn	95.7 Al 0.44 Mn 3.94 Cu	–	–	85.7 Al 8.6 Ti 1.27 Cu 0.41 Cd 3.98 La **$Al_{6.0}$(Ti, La, Cu, Cd)**	–	–	79.3 Al 1.23 Ti 0.48 Mn 13.5 Cu 0.21 Cd 5.32 La 0 Fe **$Al_{3.83}$(Cu, La, Ti, Cd, Mn)**	78.4 Al 0.32 Mn 0.27 Fe 20.5 Cu 0.5 Cd **$Al_{3.63}$(Cu, Cd, Mn, Fe)**

Note. The components are underlined.

until t_q = 605 °C. Consequently, the maximum total solubility of copper and manganese in the α_2-solid solution is reached at 545 °C. At the quenching temperature of 585 °C, only an increased copper content in the α_2-solid solution is observed. As a result, higher microhardness of the α-solid can be anticipated at these quenching temperatures.

Table 3 indicates that segregation increases with the quenching temperature, impacting the stoichiometry of the crystallized metal aluminides. Aluminides with La additions ($Al_xTi_yLa_zCu_vCd_w$) most commonly crystallize at t_q = 545÷605 °C. Notably, $Al_{4.12}$(Cu, Ti, Mn) aluminides, containing 9.09 at. % of Ti and 9.22 at. % of Cu, form at the 585 °C quenching temperature. Additionally, $Al_{3,63}$(Cu, Cd, Mn, Fe) is formed at t_q = 605 °C (refer to Table 3).

For the $Al_xTi_yLa_zMn_vCd_w$ alloyed aluminide, the highest solubility of the additions (Cu, La, Ti) occurs at t_q = 585 °C. In this aluminide, the Cd content decreases, while the Al content increases (Fig. 5, *c*).

Microhardness measurements of the $Al_xTi_yLa_zMn_vCd_w$ aluminides are presented in Fig. 5, *c*.

The AM4.5Kd + 0,2 wt.% La alloy exhibits its maximum hardness (98—104 HB) at quenching temperatures of 535—545 °C. At t_q = 605 °C, the hardness drastically drops to ~60 HB (Fig. 6, *a*). The maximum microhardness of the base metal (α-solid solution) is achieved at t_q = 535÷545 °C, reaching ~150 HV (Fig. 6, *b*).

Fig. 2, 4, and Table 1, 2 illustrate that all the intermetallides, except for the complex $Al_xTi_yLa_zMn_vCd_w$ alloyed aluminide, exhibit a dispersed structure, preventing the measurement of their microhardness.

The microhardness of the $Al_xTi_yLa_zMn_vCd_w$ alloyed aluminide is 760 HV at t_q = 535÷545 °C and it drops to 660 HV at t_q = 605 °C (Fig. 6, *c*).

Consequently, the maximum total hardness of the alloy is observed at 535—545 °C, primarily due to the high microhardness of the α-solid solution with its elevated Cu and Mn content. There appears to be a relationship between the variations in hardness for the AM4.5Kd + + 0.2 wt.% La alloy, the microhardness of the α-solid solution, the complex $Al_xTi_yLa_zMn_vCd_w$ alloyed aluminide, and their respective compositions.

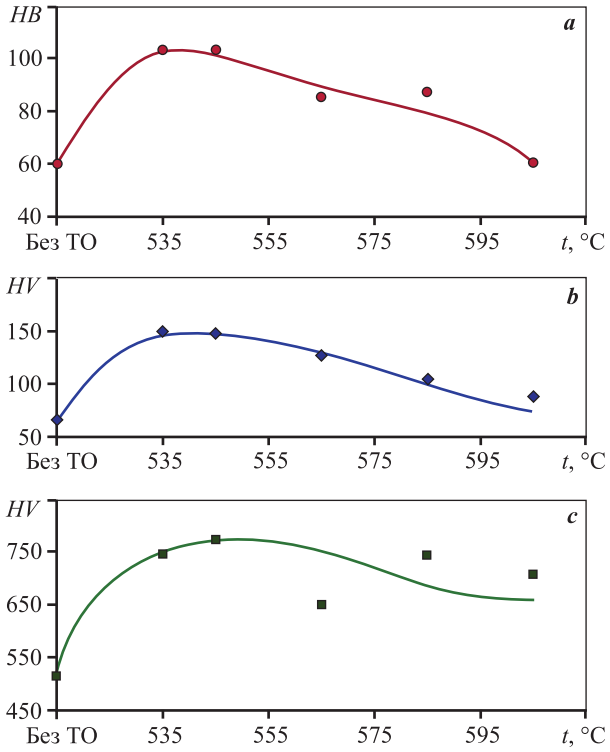

Fig. 6. Quenching temperature vs. the hardness of the AM4.5Kd + 0.2 wt.% of La alloy (***a***), α-solid solution microhardness (***б***), and $Al_xTi_yLa_zMn_vCd_w$ alloyed aluminide microhardness (***в***)

Рис. 6. Влияние температуры закалки на твердость сплава АМ4,5Кд + 0,2 мас.% La (***а***) и микротвердость α-твердого раствора (***б***) и легированного алюминида типа $Al_xTi_yLa_zMn_vCd_w$ (***в***)

Conclusion

1. An increase in the quenching temperature from 535 to 605 °C, followed by aging at 155 °C for 4 h, promotes the enlargement of structural components, including the α-solid solution, metal aluminides, and eutectics.

2. XRD elemental analysis identified the structural components of the AM4.5Kd + 0.2 wt.% of La for various quenching temperatures.

3. The base metal (α-solid solution) exhibits nonhomogeneity in its chemical composition. The contents of Cu and Mn in the α_1-solid solution decrease from 2.6 at.% of Cu and 2.5 at.% of Mn at 535 °C to 1.27 at.% of Cu and 0.44 at.% of Mn at 605 °C. The Cu and Mn solubility in the α_2-solid solution depends on the quenching temperatures. The maximum Cu (4.5 at.%) and Mn (4.25 at.%) contents occur at t_q = 545 °C. The α_2-solid solution has a second peak of Cu content (8.7 at.%) at t_q = 585 °C, and the Mn content at t_q = = 585 °C is 1.0 at.%.

4. Aluminides of alloying elements with different stoichiometries crystallize at different quenching temperatures. Complex $Al_xTi_yLa_zCu_vCd_w$ и $Al_xCu_yMn_zCd_v$ alloyed aluminides are most commonly found in the 545—605 °C quenching temperature range. The highest content of Cu, Ti, and La additions in the $Al_xTi_yLa_zCu_vCd_w$ aluminide occurs at 585 °C, where

the Cd content decreases, and that of Al increases at $t_q = 605$ °C.

5. Increasing the quenching temperature to 535—545 °C results in a higher hardness of the AM4.5Kd + + 0.2 wt.% of La alloy, reaching to 98—104 HB, with subsequent decrease to 60 HB as the quenching temperature reaches 605 °C. The hardness of the unhardened alloy is 60 HB.

6. A relationship was identified between the alloy hardness, microhardness of the α-solid solution, microhardness of the complex $Al_xTi_yLa_zCu_vCd_w$ alloyed aluminide, and their compositions.

7. The optimal quenching temperature t for the AM4.5Kd alloy is 535—545 °C. This temperature corresponds to the highest hardness of the alloy and the $Al_xTi_yLa_zMn_vCd_w$ alloyed aluminide.

References

1. Ogorodov D.V., Trapeznikov A.V., Popov D.A., Pentyukhin S.I. Development of foundry aluminum alloys in VIAM (to the 120th anniversary of the birth of I.F. Kolobnev). *Trudy VIAM*. 2017;2(50):105—122. (In Russ.).
Огородов Д.В., Трапезников А.В., Попов Д.А., Пентюхин С.И. Развитие литейных алюминиевых сплавов в ВИАМ (к 120-летию со дня рождения И.Ф. Колобнева). *Труды ВИАМ*. 2017;2(50):105—112.
2. Belov N.A., Alabin A.N. Promising aluminum alloys with increased heat resistance for reinforcement engineering as a possible alternative to steels and cast iron. *Armaturostroenie*. 2010;2(65):50—54. (In Russ.).
Белов Н.А., Алабин А.Н. Перспективные алюминиевые сплавы с повышенной жаростойкостью для арматуростроения как возможная альтернатива сталям и чугунам. *Арматуростроение*. 2010;2(65):50—54.
3. Kvasova F.I., Fridlyander I.N. Industrial aluminum alloys. Moscow: Metallurgiya, 1984. 528 p. (In Russ.).
Квасова Ф.И., Фридляндер И.Н. Промышленные алюминиевые сплавы. М.: Металлургия, 1984. 528 с.
4. Alieva S.G., Al'tman M.B., Ambartsumyan S.M. Industrial aluminum alloys. Moscow: Metallurgiya, 1984. 527 p. (In Russ.).
Алиева С.Г., Альтман М.Б., Амбарцумян С.М. Промышленные алюминиевые сплавы. М.: Металлургия, 1984. 527 с.
5. Patel N., Joshi M., Singh A., Pradhan A.K. Effect of solution heat treatment on microstructure and some properties of Al—Cu—Mg alloy. *Transactions of the Indian Institute of Metals*. 2023;76(10):2681—2689.
https://doi.org/10.1007/s12666-023-02961-x
6. Aryshensky E.V., Aryshensky V.Yu., Drits A.M., Grechnikov F.V., Ragazin A.A. Thermal treatment effect on the mechanical properties of 1570, 1580 and 1590 aluminum alloys. *Vestnik of Samara University. Aerospace and Mechanical Engineering*. 2022;21(4):76—87. (In Russ.).
https://doi.org/10.18287/2541-7533-2022-21-4-76-87
Арышенский Е.В., Арышенский В.Ю., Дриц А.М., Гречников Ф.В., Рагазин А.А. Влияние режимов термической обработки на механические свойства алюминиевых сплавов 1570, 1580 и 1590. *Вестник Самарского университета: Аэрокосмическая техника, технологии и машиностроение*. 2022;21(4):76—87.
7. Korotkova N.O., Belov N.A., Timofeev V.N., Motkov M.M., Cherkasov S.O. Influence of heat treatment on the structure and properties of an Al—7% REM conductive aluminum alloy casted in an electromagnetic crystallizer. *Physics of Metals and Metallography*. 2020;121(2):173—179.
https://doi.org/10.31857/S0015323020020096
Короткова Н.О., Белов Н.А., Тимофеев В.Н., Мотков М.М., Черкасов С.О. Влияние режима термической обработки на структуру и свойства проводникового алюминиевого сплава Al—7%РЗМ, полученного литьем в электромагнитном кристаллизаторе. *Физика металлов и металловедение*. 2020;121(2):200—206.
8. Paitova O.V., Bobruk E.V., Skotnikova M.A. Optimization of the structure and properties of the Al—Cu—Mg system aluminum alloy. *Journal of Instrument Engineering*. 2020;63(5):476—482. (In Russ.).
https://doi.org/10.17586/0021-3454-2020-63-5-476-482
Паитова О.В., Бобрук Е.В., Скотникова М.А. Оптимизация структуры и свойств алюминиевого сплава системы Al—Cu—Mg. *Известия высших учебных заведений. Приборостроение*. 2020;63(5):476-482.
9. Zenin M.N., Guryev A.M., Ivanov S.G., Guryev M.A., Chernykh E.V. Influence of high-temperature annealing of aluminum alloys AMg6 and V95 on their structural-phase state and strength properties. *Fundamental'nye Problemy Sovremennogo Materialovedenia (Basic Problems of Material Science (BPMS))*. 2022;19(1):106—114. (In Russ.).
https://doi.org/10.25712/ASTU.1811-1416.2022.01.012
Зенин М.Н., Гурьев А.М., Иванов С.Г., Гурьев М.А., Черных Е.В. Влияние высокотемпературного отжига алюминиевых сплавов АМг6 и В95 на их структурно-фазовое состояние и прочностные свойства. *Фундаментальные проблемы современного материаловедения*. 2022:19(1):106—114.
10. Zhou W.B., Teng G.B., Liu C.Y., Qi H.Q., Huang H.F., Chen Y., Jiang H.J. Microstructures and mechanical properties of binary Al—Zn alloys fabricated by casting

and heat treatment. *Journal of Materials Engineering and Performance*. 2017;26:3977—3982. https://doi.org/10.1007/s11665-017-2852-y

11. Tan E. Change in the wear characteristics of T6 heat-treated 2024, 6063, and 7075 alloys at different quenching temperatures. *Journal of Materials Engineering and Performance*. 2023;32:1—13. https://doi.org/10.1007/s11665-023-08177-w
12. Anjabin N. Modeling the age-hardening process of aluminum alloys containing the prolate/oblate shape precipitates. *Metals and Materials International*. 2021;27:1620—1630. https://doi.org/10.1007/s12540-019-00579-7
13. Alexandrov A.A., Butorin D.V., Daneev R.A., Livshits A.V. Error estimation of the heat transfer coefficient determination devices based on mathematical modeling. *Vestnik RGUPS*. 2019;(4):8—16. (In Russ.).
Александров А.А., Буторин Д.В., Данеев Р.А., Лившиц А.В. Система компьютерного моделирования термических остаточных напряжений. *Вестник Ростовского государственного университета путей сообщения*. 2019;(4):8—16.
14. Krivopalov I.V., Baturin A.P., Erisov Ya.A. Application of computer simulation to determine the influence of quenching parameters on the geometry of parts from AK6 aluminium alloy. *Izvestiya Samarskogo Nauchnogo Tsentra Rossiiskoi Akademii Nauk*. 2021:23(6):5—9. (In Russ.).
https://doi.org/10.37313/1990-5378-2021-23-6-5-9
Кривопалов И.В., Батурин А.П., Ерисов Я.А. Применение компьютерного моделирования для определения влияния параметров закалки на геометрию штамповок из алюминиевого сплава АК6. *Известия Самарского научного центра Российской академии наук*. 2021:23(6):5—9.
15. Hu Y., Wang G., Ye M., Wang S., Wang L., Rong Y. A precipitation hardening model for Al—Cu—Cd alloys. *Materials & Design*. 2018;151:123—132. https://doi.org/10.1016/j.matdes.2018.04.057
16. Hu Y., Wang G., Ji Y., Wang L., Rong Y., Chen L.Q. Study of θ'precipitation behavior in Al—Cu—Cd alloys by phase-field modeling. *Materials Science and Engineering: A*. 2019;746:105—114. https://doi.org/10.1016/j.msea.2019.01.012
17. Liu X., Wang G., Hu Y., Ji Y., Rong Y., Hu Y., Chen L.Q. Multi-scale simulation of Al—Cu—Cd alloy for yield strength prediction of large components in quenching-aging process. *Materials Science and Engineering: A*. 2021;814:141223. https://doi.org/10.1016/j.msea.2021.141223
18. Choudhary C., Bar H.N., Arif S. Sahoo K.L., Mandal D. Effect of structural refinement and modification on the mechanical properties of Al—7Si alloy. *Journal of Materials Engineering and Performance*. 2023;1—13. https://doi.org/10.1007/s11665-023-08313-6
19. Ruan Q., Meng C., Xie Z., Tao Z., Wu J., Peng Y., Tang H., Chen P. Effect of $(Ti+V)B_2$ on the grain structure of Al—7Si alloy. *Transactions of the Indian Institute of Metals*. 2023;76(10):2765—2771. https://doi.org/10.1007/s12666-023-02954-w
20. Sahin H., Dispinar D. Effect of rare earth elements erbium and europium addition on microstructure and mechanical properties of A356 (Al—7Si—0.3Mg) alloy. *International Journal of Metalcasting*. 2023;17(4):2612—2621. https://doi.org/10.1007/s40962-023-01060-3
21. Laponogova P.A., Kolisova M.V., Goncharov A.V., Dzuyba G.S. The application of scandium for the modification of aluminum alloys on the example of 2003 aluminum alloy. In: *Innovative technologies in foundry production*. Moscow: IIU MGOU, 2019. P. 75—78. (In Russ.).
Лапоногова П.А., Колисова М.В., Гончаров А.В., Дзюба Г.С. Применение скандия для модифицирования алюминиевых сплавов на примере ВАЛ10. В сб.: *Инновационные технологии в литейном производстве*. М.: ИИУ МГОУ, 2019. С. 75—78.
22. Amer S.M., Barkov R.Y., Prosviryakov A.S., Pozdniakov A.V. Structure and properties of new heat-resistant cast alloys based on the Al—Cu—Y and Al—Cu—Er systems. *Physics of Metals and Metallography*. 2021;122(9):908-914. https://doi.org/10.31857/S0015323021090023
Амер С.М. Барков Р.Ю., Просвиряков А.С., Поздняков А.В. Структура и свойства новых литейных жаропрочных сплавов на основе систем Al—Cu—Y и Al—Cu—Er. *Физика металлов и металловедение*. 2021;122(9):977—983.
23. Bazhenov V.E., Baranov I.I., Titov A.Yu., Sannikov A.V., Ozherelkov D.Yu., Lyskovich A.A., Koltygin A.V., Belov V.D. Influence of Ti, Sr and B additions on the fluidity of A356.2 aluminium alloy. *Izvestiya. Non-Ferrous Metallurgy*. 2022;28(4):55—66. (In Russ.). https://doi.org/10.17073/0022-3438-2021-4-55-66
Баженов В.Е., Баранов И.И., Титов А.Ю., Санников А.В., Ожерелков Д.Ю., Лыскович А.А., Колтыгин А.В., Белов В.Д. Изучение влияния добавок Ti, Sr и B на жидкотекучесть алюминиевого сплава А356.2 (АК7пч). *Известия вузов. Цветная металлургия*. 2022;28(4):55—66.
24. Abramov A.A. Aluminium-titanium-boron alloying composition as an effective grain modifier for cast aluminum alloys. *Metallurgiya Mashinostroeniya*. 2021;(2):2—4. (In Russ.).
Абрамов А.А. Лигатура алюминий—титан—бор — эффективный модификатор зерна литейных алю-

миниевых сплавов. *Металлургия машиностроения*. 2021(2):2—4.

25. Andrushevich A.A., Sadokha M.A. Shrinkage phenomena in silumins when treated with long-acting modifiers. *Litiyo i Metallurgiya (Foundry Production and Metallurgy).* 2022;(3):30—35. (In Russ.).
https://doi.org/10.21122/1683-6065-2022-3-30-35
Андрушевич А.А., Садоха М.А. Усадочные явления в силуминах при обработке модификаторами длительного действия. *Литье и металлургия.* 2022;(3):30—35.
26. Shlyaptseva A.D., Petrov I.A., Ryakhovsky A.P. Complex modification of industrial silumins. *Teoriya i Tekhnologiya Metallurgicheskogo Proizvodstva*. 2021;1(36):4—10. (In Russ.).
Шляпцева А.Д., Петров И.А., Ряховский А.П. Комплексное модифицирование промышленных силуминов. *Теория и технология металлургического производства.* 2021;1(36):4—10.
27. Ri H., Ri E.H., Zernova T.S., Kalaushin M.A., Ri V.E., Ermakov M.A. Modifier: Patent 2521915 (RF). 2012. (In Russ.).
Ри Х., Ри Э.Х., Зернова Т.С., Калаушин М.А., Ри В.Э., Ермаков М.А. Модификатор: Пат. 2521915 (РФ). 2012.
28. Dobatkin V.A., Elagin V.I., Fedorov V.M. Rapidly crystallizing aluminum alloys. Moscow: VILS, 1995. 341 p. (In Russ.).
Добаткин В.А., Елагин В.И., Федоров В.М. Быстрозакристаллизующиеся алюминиевые сплавы. М.: ВИЛС, 1995. 341 с.
29. Xiao-hui Ao, Shu-ming Xing, Bai-shui Yu, Qing-you Han. Effect of Ce addition on microstructures and mechanical properties of A380 aluminum alloy prepared by squeeze-casting. *International Journal of Minerals, Metallurgy and Materials*. 2018;25(5):553—564.
https://doi.org/10.1007/s12613-018-1602-y
30. Ri E.H., Prikhodko A.A., Slavinskaya N.A. Structure forming and properties of VAL10 cast alloy modified with cerium and lanthanum. *Metallurgiya Mashinostroeniya*. 2020;(2):24—30. (In Russ.).
Ри Э.Х., Приходько А.А., Славинская Н.А. Структурообразование и свойства литейного сплава ВАЛ 10, модифицированного церием и лантаном. *Металлургия машиностроения*. 2020;(2): 24—30.

Information about the authors

Nadezhda A. Slavinskaya – Postgraduate Student of the Department of foundry production and technologies of metals of the Pacific National University (PNU).
https://orcid.org/0009-0006-6712-4923
E-mail: 2016101722@pnu.edu.ru

Hosen Ri – Dr. Sci. (Eng..), Professor of the Department of foundry production and technology of metals of PNU.
https://orcid.org/0000-0001-7633-8989
E-mail: opirus@list.ru

Ernst H. Ri – Dr. Sci. (Eng.), Head of the Department of foundry production and technologies of metals of PNU.
https://orcid.org/0000-0001-7784-1252
E-mail: 003232@pnu.edu.ru

Andrei S. Zhivetev – Cand. Sci (Eng.), Assistant Professor of the Department of foundry production and technology of metals of PNU.
https://orcid.org/0000-0003-2932-0203
E-mail: 007881@pnu.edu.ru

Информация об авторах

Надежда Александровна Славинская – аспирант кафедры «Литейное производство и технологии металлов» (ЛПиТМ) Тихоокеанского государственного университета (ТОГУ).
https://orcid.org/0009-0006-6712-4923
E-mail: 2016101722@pnu.edu.ru

Хосен Ри – д.т.н., профессор кафедры ЛПиТМ университета ТОГУ.
https://orcid.org/0000-0001-7633-8989
E-mail: opirus@list.ru

Эрнст Хосенович Ри – д.т.н., профессор, заведующий кафедрой «Литейное производство и технологии металлов» ЛПиТМ университета ТОГУ.
https://orcid.org/0000-0001-7784-1252
E-mail: 003232@pnu.edu.ru

Андрей Сергеевич Живетьев – к.т.н., доцент кафедры ЛПиТМ университета ТОГУ.
https://orcid.org/0000-0003-2932-0203
E-mail: 007881@pnu.edu.ru

Contribution of the authors

N.A. Slavinskaya – conducted experiments, performed calculations, processed results, and contributed to paper authoring.

H. Ri – formulated the problem statement, developed the research concept, authored the text, and drew conclusions.

E.H. Ri – conducted calculations, processed results.

A.S. Zhivetev – provided resources for experiments.

Вклад авторов

Н.А. Славинская – подготовка и проведение экспериментов, выполнение расчетов, обработка полученных результатов, подготовка текста статьи.

Х. Ри – формирование основной концепции, постановка цели и задачи исследования, подготовка текста статьи, формулировка выводов.

Э.Х. Ри – проведение расчетов, анализ результатов исследований.

А.С. Живетьев – планирование и проведение экспериментов, ресурсное обеспечение испытаний.

The article was submitted 12.01.2023, revised 09.11.2023, accepted for publication 13.11.2023

Статья поступила в редакцию 12.01.2023, доработана 09.11.2023, подписана в печать 13.11.2023